OBJECT-ORIENTED ASSOCIATIVE LEARNING AND RETRIEVAL WITH COMPLEX DYNAMICS

Javed I. Khan and D. Y. Y. Yun

Department of Electrical Engineering
University of Hawaii at Manoa
492 Holmes Hall, 2540 Dole Street, HI-96822
javed|dyun@hawaii.edu

Abstract

This paper presents an associative computing technique founded on the complex dynamics of optical holography which can learn given patterns as well as retrieve them from samples with localizable attention on the pattern space. Consequently, unlike existing associative memory models, this associative memory has the unique advantage of object-oriented access into its information. Localized object-oriented access is important for any form of visual image retrieval. This paper presents the theory and characterization test results of this memory with emphasis on object oriented learning.

Key words: *associative memory, attention, imperfect information, visual query, object-oriented search.*

1. Objects, Attention and Associative Computing

This paper explores how associative computing can be used for the visual object oriented encoding and content-based retrieval in image archives [5,6]. The technique presented in this paper is based on a new computing paradigm called **multidimensional holographic associative computing (MHAC)** which can perform object oriented image encoding and query based on similarity of objects in a sample image.

Content-based retrieval (or pictorial query-by-example) refers to a process where images are identified from a part of it. This part generally refers to an object or a group of objects that is useful to users' applications. The match is based on the similarity between these objects.

Parallel and distributed models of *artificial associative memory* (AAM) have demonstrated the ability to graciously cope with the inherent imprecision of image information [4,1]. They are adaptive, computationally efficient and their mode of computation is highly parallel and distributed. It has long been anticipated (almost from the days of the advent of neuro computing) that AAMs can be potentially used for content-based retrieval of image information. However, no such system has actually been implemented yet.

One of the reasons for the lack of success is that current AAMs do not have the ability to focus on visual objects or more specifically on any "meaningful" subset of the pixels in the images denoting the visual object(s). During encoding, these models nonchalantly assume all the pixels in the image as equi-important. During query, they emulate a similar indiscriminate **statistical pixel-to-pixel** distance evaluation (mean square error, entropy etc.) giving equal importance to all the pixels in the sample image. Neither the encoder nor the searcher has any control over the importance of the pixels to draw attention to any particular subset of pixels, which makes current AAMs rather simplistic to be used for image retrieval.

Attention in Encoding: The meta-control over the importance of pixels is critical for any search based on object similarity both during encoding and recalling. As an example, in a CT-scan image, a not so cognitive-wise significant region (such as empty outside) can be statistically quite dominant for its large cover, while an organ with important cognitive significance may be statistically insignificant for its small size. Logically, such a problem can be alleviated by encoder's prior-knowledge on the cognitive importance of the segments. But any matching strategy, which can not accommodate such meta importance but relies solely on the statistical importance of a feature or object (such as conventional AAMs) can not handle these situations.

Attention in Decoding: The ability to focus during query is also critical. A sample image can be interpreted in numerous ways based on the visual object(s) in it that the searcher wants to emphasize as a basis for similarity. Each interpretation may result in different answers. For example, in a sample CT image depicting an abdominal cross-section the searcher may choose either the "spinal column" or a "tumor" as his/her basis of similarity. But, current AAM models cannot accommodate such dynamic (post-learning) specification of focus. It always converges only to the statistically closest match based on all the pixels of the sample. One of the consequences of such inability to focus, is that the cues must be statistically significant, which is also unrealistic. In Conventional AAMs the cue is required to be at least 50% of the query frame for correct retrieval [6,11]. The critical index objects used in image search as a cue are always based on their cognitive importance irrespective of their statistical dominance. Such a cue is quite often only a fraction of the entire image.

In this paper a computational mechanism will be shown which can provide this critical ability of attention both during learning as well as dynamically during recall. This paper explains its operations both analytically and with an experimental implementation, with special focus on its ability to accommodate attention during learning.

2. Holographic Memory

Multidimensional Holographic Associative Computing (MHAC), inspired by optical holographic, has this critical ability to focus and thus it introduces a search capability into associative computing which is analogous to object based search of conventional database. It can overcomes the above mentioned limitations of conventional AAMs. It also retains the usual advantages of associative computing (adaptability, efficiency, ability to cope with imprecision, parallel and distributed mode of computation).

This new memory model is based on a formalism which assumes the *trust* in each piece of transacted information as inherently non-conformal (thus enabling it to handle selective and dynamically changeable attention). In addition to the basic *measurements*, the formalism includes the *meta-information* about the status of each given piece of measurements as an integral part of its representation and computation. A conventional AAM computes only with the former. Internally, the information is represented as multidimensional complex numbers (MCN) spanned in a hyperspherical space. The phase set of MCN represents the measurements while the magnitude represents the meta-information. The computational model is physically a conceptual generalization of optical holographic principles [3] and computationally an instance of associative memory.

2.1 Bimodal Associative Memory

Let a stimulus pattern is denoted by a symbolic vector $S^{\mu} = \{s_1^{\mu}, s_2^{\mu}, \ldots. s_n^{\mu}\}$. Each of the individual elements in this vector represents a piece of *information* (subscript refers to the element index and superscript refers to pattern index). The values of these elements correspond to a measurement obtained by some physical sensor.

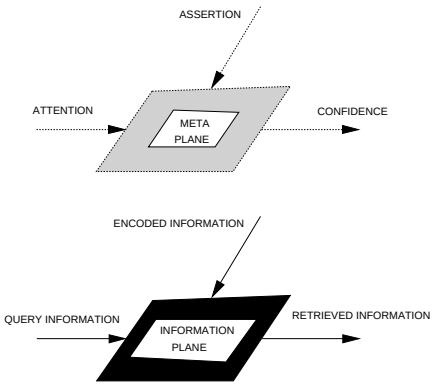

Fig-1 Information Flow Model of Bimodal Memory

A general memory has three information channels (as shown in the bottom plane of Fig-1). The first is the encoder, where information is received during learning. The second is the decoder, where query template information is received from inquirer. The third is the output channel, where for each query, the memory generates the response.

A conventional memory processes only the above measurement components of the involved information elements. In contrast, the novel formalism we would like to propose adopts an additional meta-knowledge plane (as shown in the upper plane in Fig-1) to accommodate dynamic attention.

Thus, in this new formalism each information element is modeled as a bi-modal pair $s_k^{\mu} = \{\alpha_k^{\mu}, \beta_k^{\mu}\}$. Where α represents the *measurement* of the information elements and β represents the *meta-knowledge* associated with it. The linguistic interpretation to the quantities of this meta-plane varies depending on the channel. For the encoding channel this meta-knowledge corresponds to a form of *assertion* from the encoder. For the query pattern it corresponds to a form of *attention* on the part of inquirer. For the memory response it corresponds to the *confidence* on the retrieved information as assessed by the memory itself. These terms will be used hereafter in this paper. Next section now shows how a memory based on holographic representation can realize such a bimodal memory.

2.2 Computational Representation

In optical holography an element of the pattern is represented as optical waveforms which is a 2D complex value. We adopt a generalized formalism and represent the elements in the form of *multidimensional complex numbers* (MCN) as a point on the surface of a hypersphere. In this formalism the MCN phase represents the *measurement* and magnitude represents the *meta-knowledge* component of each piece of information. Thus:

$$s_k = (\alpha_k, \beta_k) \Rightarrow \lambda_k e^{\left(\sum_j^{d-1} \hat{i}_j \theta_{j,k}\right)} \ldots. \quad (1)$$

Here, each α_i^k is mapped onto an angular span defined by the phase elements θ_i^k in the range of $\pi \geq \theta \geq \pi$ through a suitable transformation, where each $s(\lambda_k, \theta_1^k, \theta_2^k, \ldots \theta_{d-1}^k)$ is a d-dimensional vector. Each of the θ_j^k is the spherical projection (or phase component) of the vector along the dimension $\hat{i}_j$. λ_k becomes the magnitude of this vector. Thus, a stimulus with *n* elements and a response with *m* elements are represented respectively as:

$$[S^{\mu}] = \left[\lambda_1^{\mu} e^{\left(\sum_j^{d-1} \hat{i}_j \theta_{j,n}^{\mu}\right)}, \lambda_2^{\mu} e^{\left(\sum_j^{d-1} \hat{i}_j \theta_{j,n}^{\mu}\right)}, \ldots. \lambda_n^{\mu} e^{\left(\sum_j^{d-1} \hat{i}_j \theta_{j,n}^{\mu}\right)} \right]$$

$$[R^{\mu}] = \left[\gamma_1^{\mu} e^{\left(\sum_j^{d-1} \hat{i}_j \phi_{j,1}^{\mu}\right)}, \gamma_2^{\mu} e^{\left(\sum_j^{d-1} \hat{i}_j \phi_{j,2}^{\mu}\right)}, \ldots. \gamma_m^{\mu} e^{\left(\sum_j^{d-1} \hat{i}_j \phi_{j,m}^{\mu}\right)} \right]$$

Here, in the response pattern the phasor ϕ represents the measurement of the expected associated response pattern elements from the memory system, and γ represents the expected system confidence on ϕ.

2.3 Encoding

The association between each individual stimulus and its corresponding response is computed as following:

$$[X^{\mu}] = [\overline{S}^{\mu}]^T \cdot [R^{\mu}] \quad \ldots.(2)$$

The associations derived from a set of stimuli and a set of corresponding responses are superimposed on a super matrix X which is referred as Holograph.

$$[X] = \sum_{\mu}^{P} [X^{\mu}] = \sum_{\mu}^{P} [\overline{S}^{\mu}]^T [R^{\mu}] \quad \ldots.(3)$$

2.4 Retrieval

During recall, an excitory stimulus pattern $[S^e]$ is obtained from the query pattern:

$$[S^e] = \left[\lambda_1^e e^{\left(\sum_j^{d-1} i_j \theta_{j,1}^e\right)}, \lambda_2^e e^{\left(\sum_j^{d-1} i_j \theta_{j,2}^e\right)}, \ldots. \lambda_n^e e^{\left(\sum_j^{d-1} i_j \theta_{j,n}^e\right)} \right]$$

The decoding operation is similarly performed as following:

$$[R^e] = \frac{1}{c} [S^e] \cdot [X] \qquad where, \quad c = \sum_k^n \lambda_k \quad \ldots.(4)$$

The basic associative memory characteristics of this model explaining how equations (2), (3), and (4) together can correctly retrieve original stored response despite superimposition of the associations in (3) is given in [6].

As expected, this new computational model has advantages similar to the conventional AAMs. In fact, as shown in equation (4), a search into thousands of stored images through this technique requires a single complex matrix multiplication. Now, the capability of assertion and attention control is explained next.

3. Attention and Assertion

3.1 Basics

By combining the encoding and decoding operations expressed in equations (3) and (4), the retrieved association is given by equation (5). Here, the retrieved response is decomposed into two components, one is the *principal component*, which is the response generated from the association which is closest to the query stimulus S^e. The other is the *crosstalk component*, which represents the effect generated from rest of the associations.

$$[R^e] = \frac{1}{c} \cdot [S^e]\,[\overline{S^t}]^T\,[R^t] + \frac{1}{c} \cdot \sum_{\mu \neq t}^{P} [S^e]\,[\overline{S^\mu}]^T\,[R^\mu] = [R^e_{principal}] + [R^e_{crosstalk}] \quad \ldots.(5)$$

Here S^t represents the candidate match. The specific characteristics for the crosstalk and the principal components are derived next.

3.2 Principal Component

Lemma 1: *If, the excitatory stimulus S^e, bears type-U similarity to any priory encoded stimulus S^t, in their α-suit then the principal component of generated response R^e resembles its corresponding response pattern R^t.*

Proof: First, the principal component given by equation (5) will be analyzed to estimate the λ of the recalled response in terms of the closeness of the query stimulus S^e and the candidate match with a priory encoded pattern S^t. Let us consider the retrieval of the j^{th} component of the response. Other response components are retrieved independently in identical manner. It is also assumed that all the encoded stimulus pattern have $\lambda = 1$ without any loss of generality.

$$r^e_{j(principal)} = \frac{1}{c}[S^e]\,[\overline{S^t}]^T r^t_j = \frac{1}{c}\left[\lambda^e_1 e^{\left(\sum_j^{d-1} \hat{i}_j \theta^e_{j,1}\right)}, .. \lambda^e_n e^{\left(\sum_j^{d-1} \hat{i}_j \theta^e_{j,n}\right)}\right] \begin{bmatrix} \lambda^t_1 . e^{\left(-\sum_j^{d-1} \hat{i}_j \theta^t_{j,n}\right)} \\ \lambda^t_2 . e^{\left(-\sum_j^{d-1} \hat{i}_j \theta^t_{j,n}\right)} \\ \cdot \\ \cdot \\ \cdot \\ \cdot \\ \lambda^t_m . e^{\left(-\sum_j^{d-1} \hat{i}_j \theta^t_{j,n}\right)} \end{bmatrix} r^t_j$$

$$= \frac{1}{c} \sum_k^n \lambda^t_k \cdot \lambda^e_k \cdot e^{\left(\sum_j^{d-1} \hat{i}_j \left(\theta^e_{j,k} - \theta^t_{j,k}\right)\right)} \cdot r^t_j \quad \ldots(6)$$

If, the query stimulus, and the target stimulus corresponds closely, then $\theta^t_{j,k} \rightarrow \theta^e_{j,k}$. Thus, all the exponent terms become unity with no phase disturbance. Which, reduces to,

$$r^e_{j(principal)} \cong \frac{1}{c} \sum_k^n \lambda^e_k \cdot \lambda^t_k \cdot r^t_j \quad \ldots.(7.1)$$

The phase of the retrieved response corresponds to the retrieved information, and is equivalent to the phase of the encoded response:

$$argc(r^e_{j(principal)}) \cong argc(r^t_j) \quad \ldots.(7.2)$$

.

3.3 Crosstalk Component

Lemma 2: *For sufficiently symmetrical distribution of the stimulus and response patterns, the magnitude of the crosstalk component tends to be zero.*

Proof: The crosstalk component can be thought as a summation of a set of randomly oriented d-dimensional vectors. Let us, consider uni-normal projection of a set of such vectors $\vec{A}_{\mu}^{d}$,

$$r_{crosstalk}^{e} = \frac{1}{c}.\sum_{\mu \neq t}^{P} [S^e][\bar{S}^{\mu}]^T [R^{\mu}] = \frac{1}{c}.\left\{\sum_{\mu \neq t}^{P} \vec{A}_{\mu}^{d}\right\}$$

Let the d-dimensional vector (left hand side components of equation (5)) is represented as:

$$\vec{A}_{\mu}^{d} \equiv A(\theta_1^{\mu}, \theta_2^{\mu}, \ldots \theta_{d-1}^{\mu}) \equiv A(x_1^{\mu}, x_2^{\mu}, \ldots x_d^{\mu})$$

If the phases are symmetrically distributed, i.e., the distribution functions $f_{\theta}(x) = f_{\theta}(\pi - x)$ in the $0 - 2\pi$ range, then,

$$E\{\cos\theta\} = \int \cos x\, f_{\theta}(x) dx \rightarrow 0 \qquad E\{\sin\theta\} = \int \sin x\, f_{\theta}(x) dx \rightarrow 0$$

Which implies that,

$$r_{crosstalk}^{e} = \frac{1}{c}.\left\{\sum_{\mu \neq t}^{P} \vec{A}_{\mu}^{d}\right\} \cong 0 \qquad \ldots.(proved)$$

It should be noted that for effective operation the magnitude of the cross-talk component should be kept sufficiently small compared to the principal component in practice. The actual value of this term depends on (i) the distribution function $f_{\theta}()$ and (ii) average magnitude of $\vec{A}_{\mu}^{d}$s. Symmetrical distribution of the vectors and lower assertion values tends to keep the saturation low.

The above two lemmas together explain how the above computation mechanism can act as an associative memory.

3.4 Attention and Assertion Characteristics

Lemma 3 (Assertion Control): *Given a encoded stimulus S^t with unequal analog distribution of assertion of its element field specified by $\Lambda^t = [\lambda_1^t, \lambda_2^t, \ldots, \lambda_n^t]$, and the memory dynamics specified by equations (3) and (4), the elements of the target pattern will contribute in the reconstruction of the target pattern $r_{j(principal)}^{e}$ in monotonic proportion based on the weighted importance specified in Λ^t.*

Lemma 4 (Attention Control): *Given a query stimulus S^e, with unequal analog distribution of attention distribution of its element field specified by $\Lambda^e = [\lambda_1, \lambda_2, \ldots, \lambda_n]$, the memory dynamics specified by equations (3) and (4) retrieves the pattern which best resembles S^e, where, individual query elements contributes in the matching in monotonic proportion based on the weighted importance specified in Λ^e.*

Proofs: The proof is straightforward. As evident in (5), the phase of the reconstructed response $r_{j(principal)}^{e}$ is in effect a weighted average of the individual encoded responses r_j^t associative with individual element locations where the contribution of each term is weighted by both λ_k^t and λ_k^e. ... *(proved).*

Lemmas 1 and 2 together shows how the above computational mechanism works as an associative memory. Lemmas 3 ans 4 explain the attention and assertion control mechanism of it. By adjusting individual λ_k^t's the contribution of each encoded stimulus element can be controlled during learning. A high λ_k^t will allow the k^{th} term to contribute more in the phase average, and vice versa. At the extreme, setting λ_k=0 will completely attenuate this term. But, such analog control will have no multiplicative distortion effect on the phase plane. This mechanism corresponds to the process of learning with changeable assertion. In a similar way, by adjusting individual λ_k^e's the contribution of each query stimulus element can be controlled during query. This mechanism corresponds to

the process of retrieval with changeable attention. As can be noted, within the region of focus (either by assertion or attention) the match is still "statistical" like conventional AAMs. Thus, it maintains the usual error tolerance of AAMs.

4. Image Archival and Retrieval Scheme

Now we will describe a scheme for object-oriented image encoding and retrieval using MHAC. In its simplest form, a large number of image frames are first "folded" into the correlation memory substrate of MHAC, called the **holograph** using a generalized multidimensional differential Hebbian learning algorithm. The encoder can provide a fuzzy **assertion field** to specify cognitivically important regions.

The MCN learning algorithm in addition to "enfolding" the individual measurements (in the phase plane) also learns the cognitive importance of the pixel elements (in the magnitude plane).

During the visual query, similarly, the inquirer provides a sample image and a fuzzy **attention field**. The associative search mechanism of MHAC performs an associative search into the holographic repository and returns the best match with respect to the objects specified by the field. The inquirer can dynamically alter (or compound) the field to focus on any other object.

5. Test Results

Experiments were conducted to demonstrate the feasibility and evaluate the performance of this holographic archive system using a prototype medical image archive (MEDIA), which "enfolds" 64 CT-images into the holographic memory. It demonstrates the crucial role of attention in both encoding and query processes.

Assertion Based Encoding: First using a Clipped-Gaussian segmentation algorithm CT-scan/MRI images has been segmented into five segments (i) bone tissue, (ii) soft tissue, (iii) fat tissue, (iv) water and (v) air segments based on their x-ray/electromagnetic refractivity. The membership value of a pixel in a class is defined by four parameters using (8):

$$m_k = m(I_{\min}, I_{\max}, \mu, \sigma) = 1 \qquad \text{when} \qquad I_{\min} \le I_k \le I_{\max}$$

$$= e^{-\frac{(\mu - I_k)^2}{\sigma}} \qquad \text{otherwise.} \qquad \ldots.(8)$$

Fig-2 shows the result of a typical segmented image. Table-1 gives the parameter of segmentation and the cover of the corresponding regions. The assertion strength (or cover) is computed as (9):

$$f = \frac{\sum_{k=1}^{N} \lambda_k}{N} \qquad \ldots.(9)$$

The first two or three of these segments actually bear cognitive importance to a radiologist. As evident in this example, quite often the large (and statistically dominated) air surrounding the objects of focus, not only is cognitive unimportant, but quite often they create skew in the symmetry of distribution during plain associative encoding.

Table-1 Segmentation for Plate#50

Region	$I_{\max} - I_{\min}$	μ	σ	f
BONE	255-201	255	0.010	0.044
TISSUE	180-150	144	0.015	0.288
FAT	140-080	100	0.010	0.156
LIQUID	045-030	100	0.010	0.167
AIR	025-000	025	0.050	0.320

To avoid such unnecessary interference, In MHAC scheme we have "enfolded" the air image regions with very low assertion. The assertion values of individual pixels are computed from class assertion strength *AF* by (10):

$$\lambda_k^e = AF_{class} \cdot m_k \qquad \ldots.(10)$$

For comparison, the pixels of air segment has been assigned several assertion values (1,0.5, 0.1 and .01). The reduction of assertion values improved the symmetry of distribution for most of the images. Fig-3 graphically demonstrates how the asymmetry changes for each of these 64 images with the lowering of assertion. For example, for plate #50, the AF=1.0 encoding shows an asymmetry =.28, while with reduces emphasis on air segment asymmetry becomes as low as .02. Plates which do not have large air segment (such as #1, #2, #3, etc) show little change in asymmetry value.

The end results of variable assertion "enfolding" on holographic memory performance are demonstrated in Fig-4. It plots the average recall accuracy. As, evident such shielding, not only reduces the saturation of the memory but also improves the quality of recalled information by reducing the amount of interference from non-important image segments. Fig-5 plots the asymmetry and corresponding recall SNR for all these four cases as an average.

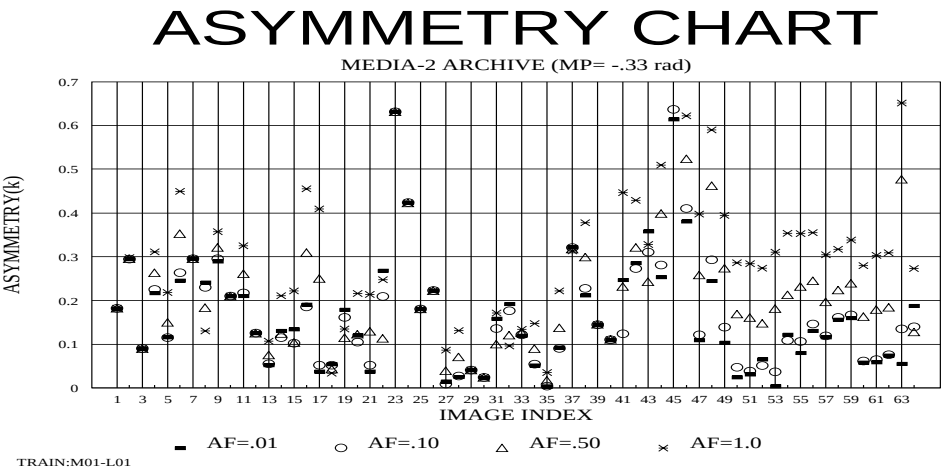

Fig-3 Asymmetry Reduction

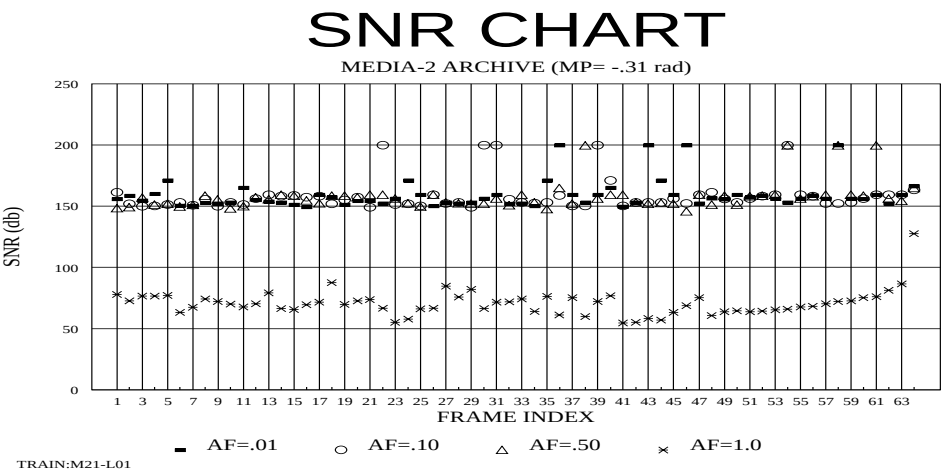

Fig-4 Recall Performance

Attention Based Retrieval: Two sets of test have been performed to characterize the attention behavior of MHAC. Fig-6 respectively show the scheme of attention windowing for these tests. Fig-7 shows the result of variable assertion encoding when during the retrieval the attention has been varied from 60x60 to 110x110 pixels in 6 steps. It is called ZOOM test. Fig-8 shows the result when the attention window has been spatially translated across different locations of the query image frame with a fixed window size of 55x55 pixels. Both of the figures plot the average retrieval accuracy in the bar-plot (left y-scale) and the corresponding size of the focus window in the line-plot (right y-scale). The three bar sets denote the accuracy for three assertion value for the air segment assumed during training.

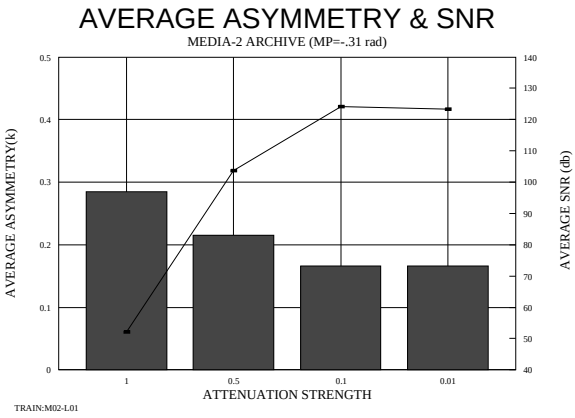

Fig-5 Average Recall Performance

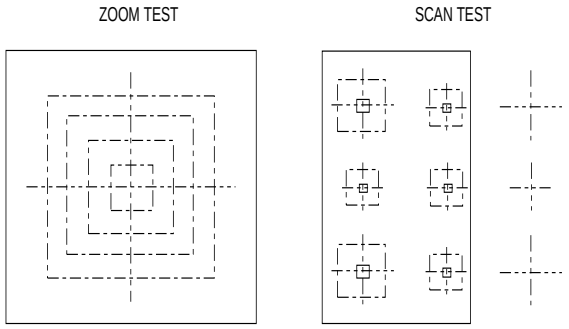

Fig-6 Characterization Tests

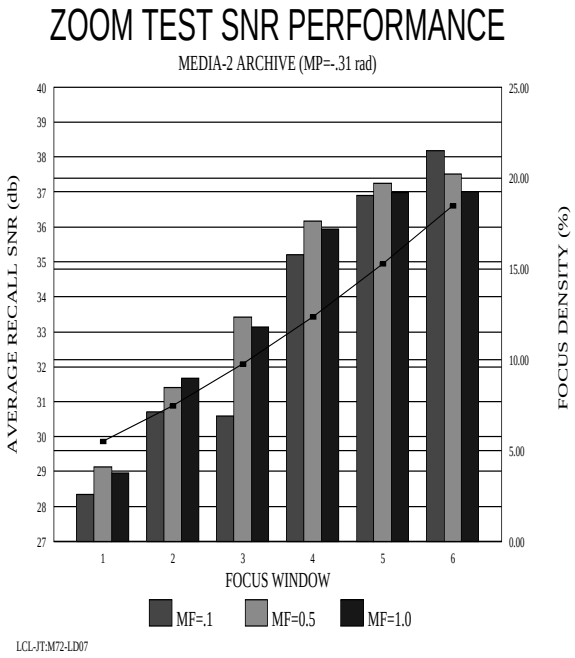

Fig-7 Zoom Test

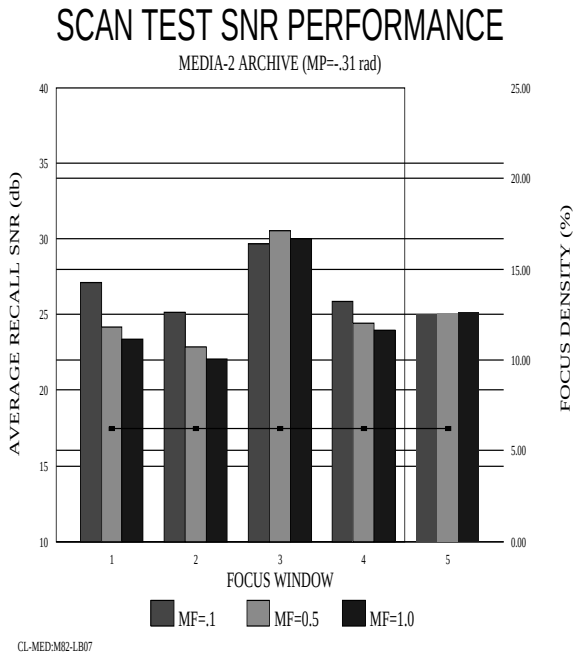

Fig-8 Scan Test

As evident, the retrieval accuracy remained well above 20-25db even for attention window lower that 10% of the total frame. Also the relationship between the performance and focus is near-linear. This is remarkably different from conventional AAMs, which show cutoff at 50% irrespective of their sophistication. Also evident in these graph is that despite the loss of information during low assertion encoding relatively little performance was lost. This is in fact due to the fact that the information that has been dropped by low assertion encoding was anyway unusable. In Fig-8 it is also evident that the accuracy of retrieval is in general high for center (number 3) window. This conforms to the general nature of CT and MRI images where the object of cognitive importance are always centered.

6. Conclusions

In terms of accuracy holographic associative search mechanism achieved almost 80-90% retrieval precision with focus as low as 10-30% of the image field, which far exceed the capabilities of any conventional AAM. As evident in equation (4) that the retrieval is a complex inner product evaluation, thus the retrieval response time is constant with respect to number of images. For the experimented database the search is about 10 times faster than an equivalent traditional database search.

Although, the principal focus of this paper is the fundamentally new capability of attention modulated learning and retrieval, multidimensional holographic associative memory model (MHAC) has also demonstrated superior convergence and capacity[1] than other AAMs (Hopfield, BAM, fuzzy-ART, etc.). For example, experiment has demonstrated that 1024 randomly generated patterns each with 4K elements can be associatively enfolded on a MHAC memory of 12K bytes and can be recalled with less than 4% error. Besides scalability on conventional parallel processors, MHAC has excellent suitability for optical processor implementation [6,8].

The general problem of content-based retrieval is an extremely complex one involving human cognizance [7,2,5]. Any single solution is far from complete. Holographic method provides only a means for efficient large scale object oriented search, and may be considered a method that supplements existing ones. In general, an associative visual search approach like MHAC will be more effective when the images tend to be natural (non-graphical), the objects are difficult to describe or model, the image volume is enormous and examples with visual similarity at the object level are available.

7. References

[1] Caudill, M. & C. Butler, *Naturally Intelligent Systems*, MIT Press, 1990.

[2] Chang, S.K., Arding Hsu, "Image Information Systems: Where Do We Go From Here?", *IEEE Trans. on Knowledge and Data Engineering*, v.4, n.5, pp431, October 1992.

[3] Gabor, D., "Associative Holographic Memories", *IBM Journal of Research and Development*, 1969, I3, p156-159.

[4] Hinton, G.E., J. A. Anderson, *Parallel Models of Associative Memory*, Lawrance Erlbaum, NJ, 1985.

[5] Iyenger, S.S., R. L. Kashyap, "Guest Editors' Introduction on Image databases", *IEEE Trans. on Software Eng.*, v.14, n.5, pp608-609, May 1988.

[6] Khan, Javed. I., "Attention Modulated Associative Computing and Content Associative Search in Images", *Ph.D. Dissertation*, Department of Electrical Engineering, University of Hawaii, July, 1995.

[7] Khan Javed. I.,& D. Y. Y. Yun, "Searching into Amorphous Information Archive", *International Conference on Neural Information Processing*, ICONIP'94, Seoul, October, 1994, pp739-749.

[8] Kumar, B. V. K. V & P. K. Wong, "Optical Associative Memories", *Artificial Neural Networks and Statistical Pattern Recognition*, I. K. Sethi and A. K. Jain (Editors), Elsevier Science Publishers, pp219-241, 1991.

[9] Masters, T., *Signal and Image Processing with Neural Networks*, John Wiley & Sons, New York, 1994.

[10] Sutherland, J., "Holographic Models of Memory, learning and Expression", *International J. Of Neural Systems*, 1(3), pp356-267, 1990.

[11] Tai, Heng-Ming, T. L., Jong, "Information Storage in High-order Neural Networks with Unequal Neural Activity", *J. of Franklin Institute*, v.327, n.1, 1990, pp16-32.

1 Previously [10] and [9] has used similar 2D complex valued representation to construct conventional associative memories (without focus ability) and also reported similar high performance of their networks. Virtually unlimited number of patterns can be enfolded on MHAC using higher order encoding.

(a) CT scanned image

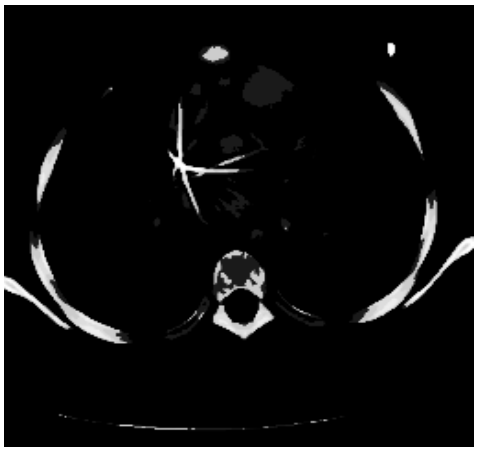

(b) Bone segment

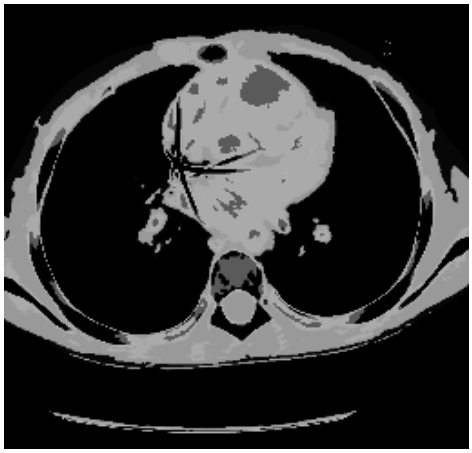

(c) Soft tissue segment

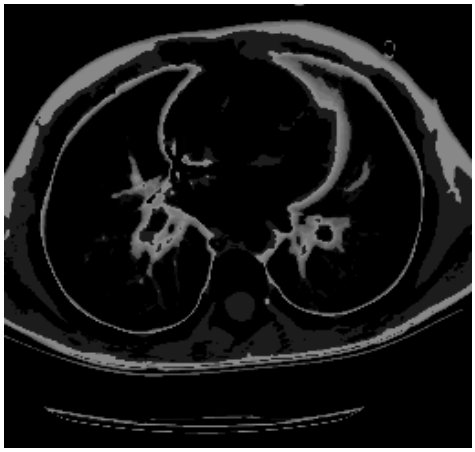

(d) Fat tissue segment

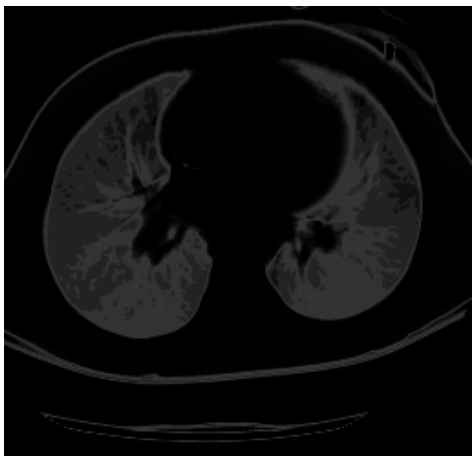

(e) Liquid segment

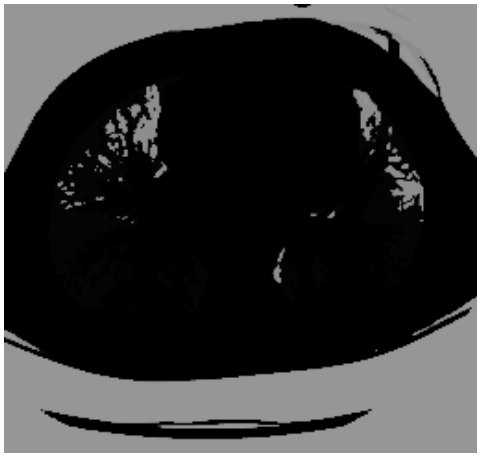

(f) Air segment(negative)

Fig-2 Clipped Gaussian Segmentation Window